Journal of ELECTRONIC MATERIALS
DOI: 10.1007/s11664-013-2884-5

Use of Atomistic Phonon Dispersion and Boltzmann Transport Formalism to Study the Thermal Conductivity of Narrow Si Nanowires

HOSSEIN KARAMITAHERI,[1,2,4] NEOPHYTOS NEOPHYTOU,[1,3,5] and HANS KOSINA[1,6]

1.—Institute for Microelectronics, TU Wien, Gußhausstraße 27-29/E360, 1040 Vienna, Austria. 2.—School of Electrical Engineering, Sharif University of Technology, 11365-9363 Tehran, Iran. 3.—School of Engineering, University of Warwick, Coventry CV4 7AL, UK. 4.—e-mail: karami@iue.tuwien.ac.at. 5.—e-mail: neophytou@iue.tuwien.ac.at. 6.—e-mail: kosina@iue.tuwien.ac.at

We study the thermal properties of ultra-narrow silicon nanowires (NW) with diameters from 3 nm to 12 nm. We use the modified valence-force-field method for computation of phononic dispersion and the Boltzmann transport equation for calculation of phonon transport. Phonon dispersion in ultra-narrow 1D structures differs from dispersion in the bulk and dispersion in thicker NWs, which leads to different thermal properties. We show that as the diameter of the NW is reduced the density of long-wavelength phonons per cross section area increases, which increases their relative importance in carrying heat compared with the rest of the phonon spectrum. This effect, together with the fact that low-frequency, low-wavevector phonons are affected less by scattering and have longer mean-free-paths than phonons in the rest of the spectrum, leads to a counter-intuitive increase in thermal conductivity as the diameter is reduced to the sub-ten-nanometers range. This behavior is retained in the presence of moderate boundary scattering.

Key words: Silicon nanowires, thermal conductivity, modified valence-force-field method, Boltzmann transport equation, low-dimensional effects

INTRODUCTION

The thermal conductivity of bulk Si is relatively high, $\kappa \approx 140$ W/mK, and is dominated by phonon transport. In low-dimensional Si nanowires (NWs), on the other hand, thermal conductivity is much lower; this is attributed to strong boundary-scattering effects.[1–3] Numerous studies of the thermal conductivity of Si NWs have been reported in the literature.[4–8] The effects of different scattering mechanisms, i.e. surface roughness scattering, mass doping, phonon–phonon scattering, and phonon–electron scattering, have been investigated by several authors.[9–12] Phonon dispersion in low-dimensional materials is, however, different from bulk dispersion. For ultra-narrow NWs, i.e. below 10 nm in diameter, the effect of confinement can further change the phonon spectrum substantially, and thus the thermal properties.

The effects of nanostructuring on the nature of phonon modes in low-dimensional channels, and on thermal conductivity, are still not well understood. It is common practice in simulation studies to use either continuum approaches or Si bulk dispersion (even in confined geometry).[7,9,13–15] Other studies use purely diffusive boundary scattering (specularity, $p = 0$),[14,16,17] or the same scattering probability for all phonon states with different wavelength (p = constant),[9,18] which is effective in explaining experimental measurements for confinement length scales down to several tens of nanometers. However, phonon mode dispersion and density of states are strongly modified in nanostructures, and atomistic

(Received June 28, 2013; accepted October 24, 2013)

Published online: 19 November 2013

description of phonon dispersion and the wave nature of phonons acquires significant importance.

In this work we used the modified valence-force-field (MVFF) method[19,20] with ballistic Landauer formalism and the diffusive Boltzmann transport equation for phonons, to address the effects of structural confinement of phonons on the thermal properties of low-dimensional Si NWs of diameter from 12 nm down to 3 nm. We showed that long-wavelength phonons are much more significant in 1D systems than they are in bulk material. Their density, and their significance compared with the rest of the spectrum, increase as the diameter is reduced, which results in more than ~60% of the heat being carried by these long-wavelength, low-energy phonons, which, in turn, undergo relatively weaker scattering.[21] This results in a counter-intuitive increase in thermal conductivity with diameter reduction, which is retained even in the presence of moderate boundary scattering. Finally, we show that, because of the specular scattering nature of the long-wavelength phonons at the boundaries under weak roughness amplitudes, a large portion of the heat is carried by phonons with mean-free-paths (MFPs) significantly larger than the NW diameter.

APPROACH

For calculation of the phononic band structure we used the MVFF method,[19] which is an extension of the Keating model.[22] In this method the interatomic potential is modeled by use of the bond deformations: bond-stretching, bond-bending, cross-bond-stretching, cross-bond-bending-stretching, and coplanar-bond-bending interactions.[19] The model accurately captures the bulk Si phonon spectrum and the effects of confinement in NWs.[20] As an empirical atomistic model, its variables are calibrated to the bulk dispersion, in this case over the entire Brillouin zone. This is common practice for electronic structure methods as well (e.g. the use of tight-binding, pseudo-potential, and k.p methods for the electronic properties of nanostructures). Transferability of the model variables for nanostructures is then assumed. Of course the only true verification is comparison with experimental measurements, which at this point are sparse for NWs, especially those with such ultra-narrow diameters. Typical phonon modes for NWs are shown in Fig. 1. Figure 1a–c show the lower energy part of the dispersions of ⟨111⟩-oriented NWs of diameters D = 12 nm, 6 nm, and 3 nm, respectively. We note that without loss in generality we use the ⟨111⟩ transport orientation in this manuscript unless otherwise specified. The phonon spectrum of the thicker NWs consists of many more modes than that for thinner NWs. The lowest four acoustic branches, however, other than some changes in their shape, remain the same as the diameter is reduced. The energy region in which only these four bands contribute is shown by the curly brackets in each NW case. Because the number of these bands remains the same, although the diameter is reduced, their density per unit of cross section area increases. As we show below, this has large consequences for the thermal conductivity of the NWs.

After calculating the phonon dispersion, the thermal conductivity was obtained by assuming the phonon relaxation time approximation in the phononic Boltzmann transport equation as:[13,23]

$$\kappa_{\mathrm{l}} = k_{\mathrm{B}} \sum_{i,q} \tau_i(q) v_{\mathrm{g},i}(q)^2 \left[\frac{\hbar\omega_i(q)}{k_{\mathrm{B}}T}\right]^2 \frac{e^{\hbar\omega_i(q)/k_{\mathrm{B}}T}}{\left(e^{\hbar\omega_i(q)/k_{\mathrm{B}}T}-1\right)^2}, \tag{1}$$

where k_{B} is the Boltzmann constant, $v_{\mathrm{g},i}$ is the group velocity of a phonon of wavevector q in subband i, given by $v_{\mathrm{g},i}(q) = \partial\omega_i(q)/\partial q$, and $\tau_i(q)$ is the scattering time. For calculation of the relaxation times, we followed the bulk formalisms for Umklapp scattering as:[9,24,25]

$$\frac{1}{\tau_{\mathrm{U}}} = B\omega_i(q)^2 T \exp\left(-\frac{C}{T}\right), \tag{2}$$

where $B = 2.8 \times 10^{-19}$ s/K and C = 140 K.[26] This is the simplest model available for Si, calibrated to the bulk thermal conductivity over a large temperature range.[26] Although the model assumes 3D phonons, it is commonly used for calculation of the thermal conductivity of nanostructures also.[9,18,26] The reason why such a model derived for 3D channels provides sufficient accuracy for nanostructures, is

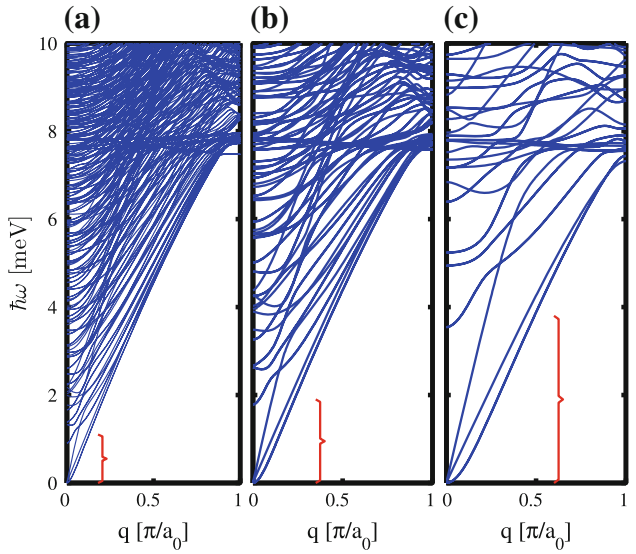

Fig. 1. Phonon dispersions for (**a**) D = 12 nm, (**b**) D = 6 nm, and (**c**) D = 3 nm NWs in the ⟨111⟩ transport orientation. As the diameter is reduced, the number of phonon modes is also reduced. The lowest four acoustic modes at low frequencies, however, remain, as indicated by the *curly brackets*.

that even for 1D channels the atomic vibrations are still in 3D and not constrained in one particular direction.[27] Modifications and extensions of this transport model to improve its validity for nanostructures, still under the assumption of 3D phonons, are described in the literature.[28,29] One of these modifications, proposed by Mingo and Broido,[27] is used here and described below. Another reason is that the dominant scattering mechanism in low-dimensional channels is boundary scattering rather than phonon–phonon scattering, and, therefore, the accuracy of the phonon–phonon scattering model will have little effect on the accuracy of the overall thermal conductivity of nanostructures.[9]

For boundary scattering we use the Casimir formula:

$$\frac{1}{\tau_{\mathrm{B},i}(q)} = \frac{1-p(q)}{1+p(q)}\,\frac{v_{\mathrm{g},i}(q)}{D}, \tag{3}$$

where D is the diameter of the NWs and $p(q)$ is the q-dependent specularity, given by:[13,21,23]

$$p(q) = \exp(-4q^2\Delta_{\mathrm{rms}}^2). \tag{4}$$

We vary the root-mean-square of the roughness amplitude as Δ_{rms} from 0.1 nm to 1.2 nm. In this model the extent of scattering depends on the confinement size D (inversely) and the specularity, p. It is again based on the assumption of 3D phonon scattering at boundaries. Although commonly used in low-dimensional nanostructures,[9,13,28] strictly speaking its validity can be questioned for ultra-narrow 1D NWs, because one cannot define a transverse phonon velocity in a purely 1D system. The model implies that the phonons are isotropic, i.e. they will travel towards the surface with the same velocity as along the wire axis. By using atomistic calculations, however, Carrete et al.,[30] have recently shown that even for ultra-thin NWs of diameter ~2 nm and with roughness amplitude as large as 20%, the phonon mean-free-path and the thermal conductivity are very close to what the Casimir limit predicts[30] (for $p = 0$). The Casimir model breaks down at much greater roughness, when strong boundary effects occur. Here, the specularity is larger for low-frequency/long-wavelength phonons, because long waves are little affected by short-range roughness. As the extent of scattering is inversely proportional to the specularity (Eq. 3), the MFPs of low-frequency phonons are longer than those of high-frequency phonons. This feature of the Casimir model is also in good agreement with atomistic calculations.[30,31] The Casimir model (Eq. 3), therefore, captures basic features of boundary-scattering down to ultra-narrow NWs, although the boundary scattering is phenomenologically different in 3D and 1D channels. In this work, however, we consider quasi-1D NWs down to $D = 3$ nm in diameter, and limit the roughness amplitude to 10% of the NWs diameter.

RESULTS AND DISCUSSION

Because the density of the low-frequency, long-wavelength phonon modes increases with diameter reduction, as mentioned above, their importance in the heat-carrying capability of the NWs increases. A simple but effective way of demonstrating this is by plotting the differential (or frequency spectrum) of the ballistic thermal conductance versus energy for NWs of different diameters, as shown in Fig. 2a.

The differential of the ballistic thermal conductance (normalized by the NW area, A) at a specific energy is calculated as:[32–34]

$$\frac{\mathrm{d}K_1(\omega)}{A\mathrm{d}\omega} = \frac{\pi k_{\mathrm{B}}{}^2 T}{6A}\sum_i \int v_{\mathrm{g},i}(q)W_{\mathrm{ph.}}(\hbar\omega)\delta(\omega-\omega_i(q))\mathrm{d}q, \tag{5}$$

where $W_{\mathrm{ph.}}(\hbar\omega)$ is the phonon window function that determines the conductance, defined as:[26,35]

$$W_{\mathrm{ph.}}(\hbar\omega) = \frac{3}{\pi^2 k_{\mathrm{B}}T}\left[\frac{\hbar\omega}{k_{\mathrm{B}}T}\right]^2 \frac{e^{\hbar\omega/k_{\mathrm{B}}T}}{\left(e^{\hbar\omega/k_{\mathrm{B}}T}-1\right)^2}. \tag{6}$$

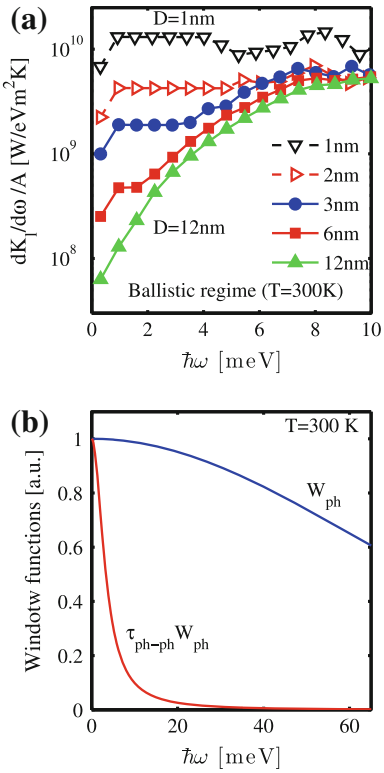

Fig. 2. (**a**) The differential contribution to ballistic thermal conductance of phonons of different energy. Nanowire diameters as they appear *from top to bottom* in the low-energy region: $D = 1$ nm, $D = 2$ nm, $D = 3$ nm, $D = 6$ nm, and $D = 12$ nm. The contribution of the low-frequency modes increases with decreasing diameter. (**b**) The phonon window function that determines the thermal conductance in the cases of ballistic (*blue*) and Umklapp-limited (*red*) scattering (Color figure online).

Under ballistic conditions, the entire energy spectrum contributes to the thermal conductance. This is contrary to what would be expected from diffusive transport, in which low-frequency modes dominate the thermal conductivity. The reason is that the phonon window function shown in Fig. 2b (blue line) is a wide and flat function at room temperature, covering most of the energy spectrum.[35] For the thicker NWs in Fig. 2a, i.e. for D = 12 nm (green-triangles), the high-frequency phonons contribute the most because the number of modes is larger at higher frequencies. As the diameter is reduced to D = 3 nm, however, although the high-frequency phonons still contribute the most, the contribution of the low-frequency modes increases. If smaller diameters are considered (D = 1 nm and 2 nm), the contribution of the low-frequency modes is even greater (note that these two curves are shown as dashed lines, to indicate what could happen, although for such low diameters we might be already reaching the limits of the transferability of the MVFF model for calculating the NW phonon dispersion). The increasing contribution of the low-frequency phonons is attributed to the fact that the density of these modes increases. Indeed, ultra-narrow NWs have a finite phonon density-of-states (DOS) at low frequencies, in contrast to the bulk, for which the phonon DOS tends to zero. A consequence of this increase in the phonon DOS at low frequencies, shown in Fig. 2a, is that their contribution to the ballistic thermal conductance increases as the NW diameter is reduced. In the paragraphs below we examine the consequences of this effect when scattering is included, and whether this increase could be retained.

Because of the finite DOS that is introduced at low-frequencies with decreasing diameter, use of the bulk model for Umklapp scattering, as in Eq. 2, causes divergence in the thermal conductivity. To avoid this divergence, either the bulk dispersion or constant specularity for phonon-boundary roughness are commonly used in the literature. This partially neglects the wave nature of phonons. However, as proposed by Mingo and Broido,[27] an additional scattering mechanism for a second-order three-phonon process (as an order of magnitude approximation) can be introduced as:

$$\frac{1}{\tau_{U2}} = A_0 T^2, \tag{7}$$

to remove this singularity for the low-frequency phonons. Here A_0 is used as a fitting term to match the extracted thermal conductivity to more sophisticated models. Use of this frequency-independent contribution for calculation of the extent of scattering is actually similar to imposing a lower-frequency cut-off in the integration over the phonon spectrum (or imposing a finite channel length as in direct methods), methods which also remove the singularity at zero frequency.

Because of this simplified treatment of second-order three-phonon processes, quantitative values for the thermal conductivity can be obtained only by fitting to more sophisticated calculations, because reliable experimental data are not available. Using a value of A_0 = 15,000/sK^2, we standardize our results to more sophisticated calculations for the thermal conductivity by Luisier,[36] who used the direct NEGF method, and Donadio and Galli,[37] who used molecular dynamics. Figure 3 shows this comparison between our calculations of thermal conductivity versus temperature (lines), those of Ref. 36 (symbols) for D = 3 nm diameter NWs in the ⟨100⟩, ⟨110⟩, and ⟨111⟩ transport orientations, and those of Ref. 37 for the ⟨100⟩ NW. The results are very similar for all three NW orientations, especially for temperatures above 200 K. The deviation is larger at lower temperatures, because our choice of A_0 was from a calibration at room temperature. A different choice of A_0 would provide a better match at lower temperatures. We should note, however, that direct comparison with Luisier's data for low temperature, at which the low-wavevector modes determine the conductivity, is not possible. Luisier's calculations used the direct method, in which the thermal conductivity depends on the length of the channel considered (up to 75 nm in that work). The longer the channel length, the more low-frequency modes participate, and the higher is the thermal conductivity. The thermal conductivity finally saturates at the diffusive value as channel length approaches infinity. This has recently been experimentally and theoretically reported for graphene nanoribbons even at room temperature.[31,38] Therefore, the higher thermal conductivity at low temperatures in our calculations compared with the work of Luisier can be partially attributed to the finite channel length used by Luisier.

The increasing importance of the long-wavelength phonons for ultra-narrow NWs is demonstrated in Fig. 4a, which shows the differential contribution to

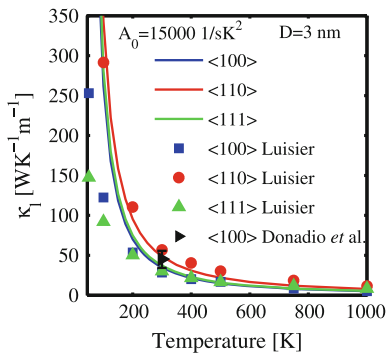

Fig. 3. Umklapp-limited thermal conductivity versus temperature for NWs with D = 3 nm in the ⟨100⟩ (*blue line*), ⟨110⟩ (*red line*), and ⟨111⟩ (*green line*) transport orientations. The *symbols* are results from calculations by Luisier[36] for the same NWs, except for the *black triangles*, which are results obtained by Donadio and Galli[37] (Color figure online).

the Umklapp-limited thermal conductivity of phonons of different frequency. We show results for three different NW diameters, D = 12 nm, 6 nm, and 3 nm. It is evident that the low-frequency phonons contribute most to the thermal conductivity. This is particularly pronounced for the narrower NWs. The thermal conductivity of phonons with energies below ~10–15 meV is almost two orders of magnitude higher than that of higher-energy phonons (note the logarithmic scale in Fig. 4a). Figure 4b shows the cumulative thermal conductivity of these NWs versus energy. Two very interesting observations can be made here:

1 Most of the contribution to the total thermal conductivity is attributed to phonons with energies below 10 meV, especially for NWs with diameters D = 3 nm and 6 nm.
2 The most interesting observation is that the Umklapp-limited thermal conductivity is larger for the thinner NWs.

The thermal conductivity of the D = 12 nm NW is reduced from the bulk value ($\kappa_{\text{bulk}} \approx 140$ W/mK) to ~15 W/mK. This is attributed to reduction of the phonon group velocity and changes in the phonon spectrum as a result of confinement.[29,39] As the diameter is reduced even further, however, the increasing contribution of the long-wavelength phonons causes the thermal conductivity to increase again. The reasons for this are:

1 The density of these modes increases compared with the rest of the spectrum as described in the ballistic results of Fig. 2a.
2 The low-frequency, low-wavevector modes undergo weaker scattering, compared with the high frequency modes.

The window function for phonon–phonon-limited transport in Fig. 2b (red line) is now (in the diffusive transport regime) multiplied by the phonon–phonon scattering lifetime as $\tau_{\text{ph.}-\text{ph.}} W_{\text{ph.}}$ (Eq. 1), which makes it a much narrower energy function, enabling mostly the low-frequency modes to participate in transport. Therefore, as the density of these important modes increases with diameter reduction, the thermal conductivity increases. We note that this counter-intuitive effect is also observed in results from more sophisticated molecular dynamics calculations by Donadio and Galli.[37] The fact that the narrowing of the phonon window function is a general feature of phonon transport explains why our simplified Umklapp model based on 3D phonons also captures (at least qualitatively) this effect, which originates from the increase in low-wavevector, low-frequency mode density. The reason why $\tau_{\text{ph.}-\text{ph.}} W_{\text{ph.}}$ is narrower than $W_{\text{ph.}}$ is because low-frequency, low-wavevector phonons have larger MFPs and relaxation times. Note that the function $\tau_{\text{ph.}-\text{ph.}} W_{\text{ph.}}$ can even be narrower if one uses the exact solution of Boltzmann transport equation. In this case, the selection rules (to ensure energy and momentum conservation) are valid only at some points of the dispersion, rather than on lines or surfaces in 2D and 3D, respectively.[27] This could indicate that in low-dimensional materials phonon–phonon scattering is weaker. Our calculations show that for the D = 1 nm NW the thermal conductivity can increase back to the bulk value (not shown), in very good agreement with molecular dynamics calculations,[37] although the accuracy of our model could be questionable at such low diameters. We should also note that this narrowing of the $\tau_{\text{ph.}-\text{ph.}} W_{\text{ph.}}$ function is not sensitive to the value of A_0 we use to calibrate our data, even if A_0 increases or decreases by an order of magnitude.

This counter-intuitive increase in the thermal conductivity with diameter reduction is also retained in the presence of phonon-boundary scattering on top of Umklapp scattering. Figure 5a, as previously Fig. 4a, shows the differential contribution to the thermal conductivity of phonons with different energies, again for NWs with diameters D = 12 nm (green), 6 nm (red), and 3 nm (blue). Compared with Fig. 4a, the inclusion of boundary scattering in Fig. 5a, reduces the differential values of the thermal conductivity but also redistributes the thermal conductivity to a much narrower energy region below 5 meV (see the peak of $d\kappa_l/d\omega$ at approximately E = 0 eV in Fig. 5a). These phonons are least affected by boundary scattering. The reason is that the specularity, $p(q)$, in Eq. 4 peaks at q = 0 indicating specular scattering, and drops

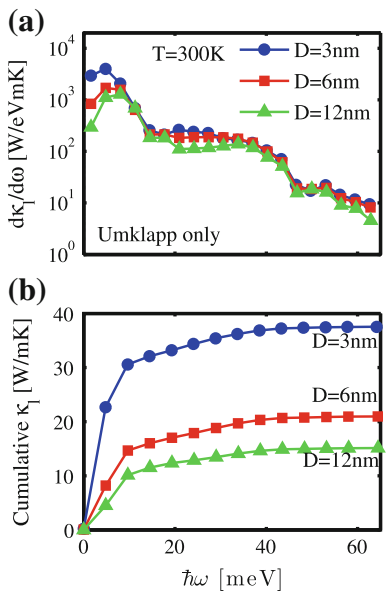

Fig. 4. (**a**) Differential contribution to the Umklapp-limited thermal conductivity of phonons of different energies. Nanowire diameters as they appear *from top to bottom* in the low-energy region: D = 3 nm, D = 6 nm, and D = 12 nm. (**b**) Cumulative thermal conductivity versus phonon energy. The thermal conductivity increases with decreasing diameter because of the increase in the contribution of low-frequency phonons which undergo less scattering (Color figure online).

sharply for higher energies. As shown in Fig. 5b (right region), although the overall thermal conductivity drops to significantly lower values, because of boundary scattering, than in Fig. 4b, the higher thermal conductivity of the D = 3 nm NW compared with the D = 12 nm NW, is still retained for small roughness amplitude (Δ_{rms} = 0.1 nm). One would have expected that the narrower the diameter, the more effectively boundary scattering reduces the thermal conductivity. This would have been true if the boundary scattering in Eq. 3 was only proportional to 1/D. The term $(1-p)/(1+p)$ in Eq. 3, however, approaches zero as p approaches unity for low-q phonons. This reduces the extent of scattering for these phonons. Because their importance increases with diameter reduction, overall scattering in the narrower NWs decreases and thermal conductivity increases. As the roughness amplitude increases, however, the increase in the Umklapp-limited thermal conductivity of the narrower NWs is lost as the boundary scattering eventually becomes stronger with decreasing NW diameter (second and third set of lines in Fig. 5b for Δ_{rms} = 0.3 nm and Δ_{rms} = 0.6 nm).

The change in thermal conductivity with decreasing dimensionality of the system is an important aspect of design for thermal management and thermoelectric applications. For thermal management in nanoscale electronic devices, a large thermal conductivity removes heat from the device and is actually desired. In thermoelectric devices, on the other hand, thermal conductivity must be reduced to retain the temperature gradient between the hot and cold sides of the device and to reduce losses. For proper design of such channels, the relevant quantity that must be taken into consideration is the MFPs of the phonons that contribute to thermal conductivity. In thermoelectric devices, for example, the design strategy used to reduce thermal conductivity is to introduce scatterers of the order of the dominant MFP.[40] The MFP of each phonon state for 1D NWs is given by the product of the phonon group velocity and relaxation time as $\lambda_i(q) = v_{g,i}(q)\tau_i(q)$. In Fig. 6a we extract the cumulative thermal conductivity versus the MFPs of the phonons for the D = 12 nm NW. We show cases for Umklapp-limited scattering (black line) and Umklapp plus boundary-limited scattering with different Δ_{rms} values for the scattering strength (Δ_{rms} = 0.1 nm, 0.3 nm, and 1.2 nm—up to 10% of the NW diameter). The red arrow indicates the 12 nm MFP, same as the diameter of the NW. For Umklapp scattering the MFPs of the phonons that contribute to thermal conductivity are distributed more or less uniformly from 1 nm to 6 μm (similar those reported for bulk Si[26,41]). The large MFPs contribute strongly to heat, as observed in the inset of Fig. 6a. Here we show a part of the phonon spectrum of this NW. The color map shows the contribution to the thermal conductivity of each of the phonon states for Umklapp-limited scattering. In red we show the large contribution to κ_l, and in blue the small contribution. The larger contribution comes from the longer MFPs of the LA branch. With the introduction of boundary scattering, on the other hand, the overall thermal conductivity is strongly reduced but the distribution of heat within the different phonon MFPs also changes. A slightly larger part of the heat compared with Umklapp-limited scattering is now carried by phonons of MFP below 12 nm, whereas long-wavelength phonons now carry less heat (Fig. 6a, right region). For small roughness amplitude, although reduced, this amount is still significant, indicating that MFPs larger than the NW diameter still contribute significantly to the thermal conductivity. For relatively strong roughness (green line, Δ_{rms} = 1.2 nm, 10% of the diameter), on the other hand, the MFPs are limited to values below the NW diameter, which indicates that the scattering approaches the Casimir limit (black-dashed line), i.e. the phonon-boundary scattering MFP is limited by the diameter of the NW. The green line in Fig. 6a, therefore, saturates after a MFP of ~12 nm. An interesting observation can be made in Fig. 6b, which shows the same quantity for the narrower NW with D = 3 nm. The Casimir limit is reached for a relatively larger percentage of roughness amplitudes (above Δ_{rms} = 0.6 nm, i.e. 20% of the NWs diameter, although this could be pushing the limits of our model). This is indicated by the fact that the green line in Fig. 6b still increases slightly for MFPs

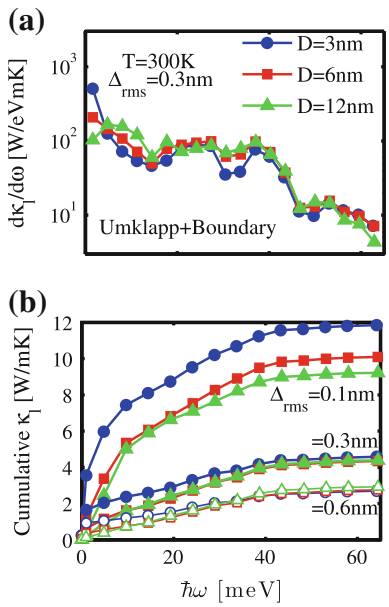

Fig. 5. (**a**) Differential contribution to the Umklapp plus boundary scattering-limited thermal conductivity of phonons of different energies. Nanowire diameters as they appear *from top to bottom* in the low-energy region: D = 3 nm, D = 6 nm, and D = 12 nm. (**b**) The cumulative thermal conductivity versus phonon energy. Cases for boundary-scattering Δ_{rms} values of 0.1 nm, 0.3 nm, and 0.6 nm are shown. For 0.6 nm, results are shown in open symbols, indicating that in this case our calculations reach the limits of the model.

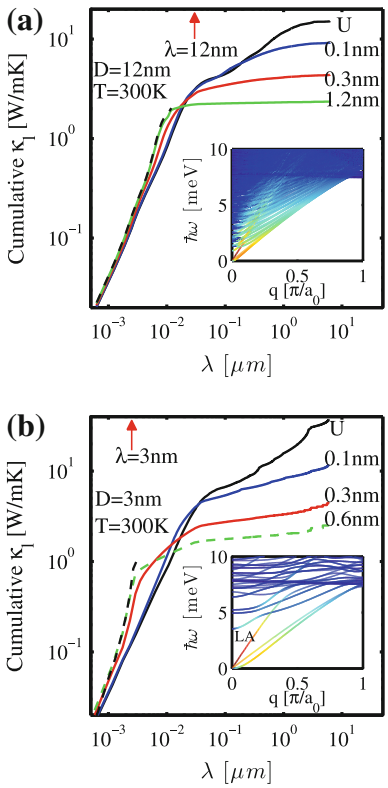

Fig. 6. Cumulative thermal conductivity of the (**a**) D = 12 nm and (**b**) D = 3 nm ⟨111⟩ NW versus MFP. Umklapp-limited thermal conductivity is shown by the *black line*. Umklapp plus boundary scattering thermal conductivity for Δ_{rms} values of 0.1 nm, 0.3 nm, and 1.2 nm are shown by the *blue*, *red*, and *green lines*, respectively, in (**a**). In (**b**) Δ_{rms} values 0.1 nm, 0.3 nm, and 0.6 nm are shown (Δ_{rms} = 0.6 nm is *dotted* as an indication, because at this value the limits of the model are reached). The MFP values of 12 nm and 3 nm, the same as the diameters of the NWs, are indicated on the *x*-axis. The fully diffusive boundary case (Casimir limit) is shown by *black-dashed lines*. *Insets*: Part of the NWs phonon dispersion, in which the color map shows the contribution of each phonon state to the total thermal conductivity (*red*: largest contribution, *blue*: smallest contribution) (Color figure online).

above ~3 nm. This is because scattering of the low-wavevector states is more specular, and, because their density in the phonon spectrum increases, the overall phonon MFP increases. It also explains why phonons with MFPs larger than the NWs diameter contribute significantly to the thermal conductivity, at least for weak roughness. Note that more sophisticated calculations at an atomistic level indicate that the Casimir limit can, indeed, describe the effect of boundary scattering in NWs of diameters even down to 2 nm and roughness amplitude even up to 20%.[30] This is quite interesting, because the Casimir formula is a simplified treatment actually based on scattering at the boundaries of 3D phonons, rather than 1D phonons.

CONCLUSIONS

In this work we studied the thermal properties of ultra-narrow silicon NWs by using the atomistic MVFF method for computation of phonon band structure and the ballistic Landauer approach and the lifetime approximation solution of the phononic Boltzmann transport equation for calculation of ballistic and diffusive thermal conductivities, respectively. We addressed the effects of structural confinement on phonon dispersion, and the consequences of this on thermal conductivity. We showed that the thermal conductivity is significantly reduced from the bulk values as the NW diameter is reduced to D = 12 nm, because of phonon band structure changes. For ultra-narrow NWs of diameters down to 3 nm, however, the thermal conductivity increases again, because of the increasing density of the long-wavelength phonons, which undergo weaker scattering. This behavior is also retained in the presence of moderate boundary scattering. Finally, we showed that a significant amount of heat in NWs is transported by phonons of MFP longer than the NWs diameter, especially in the narrowest NWs. In this case, the Casimir limit is reached for relatively large roughness of the order of 20% of the diameter.

ACKNOWLEDGEMENTS

The work leading to these results has received funding from the European Community's Seventh Framework Programme under Grant Agreement No. FP7-263306.

REFERENCES

1. A.I. Boukai, Y. Bunimovich, J. Tahir-Kheli, J.-K. Yu, W.A. Goddard, and J.R. Heath, *Nature* 451, 168 (2008).
2. A.I. Hochbaum, R. Chen, R.D. Delgado, W. Liang, E.C. Garnett, M. Najarian, A. Majumdar, and P. Yang, *Nature* 451, 163 (2008).
3. J. Lim, K. Hippalgaonkar, S.C. Andrews, A. Majumdar, and P. Yang, *Nano Lett.* 12, 2475 (2012).
4. I. Ponomareva, D. Srivastava, and M. Menon, *Nano Lett.* 7, 1155 (2007).
5. N. Yang, G. Zhang, and B. Li, *Nano Lett.* 8, 276 (2008).
6. S.-C. Wang, X.-G. Liang, X.-H. Xu, and T. Ohara, *J. Appl. Phys.* 105, 014316 (2009).
7. M. Liangraksa and I.K. Puri, *J. Appl. Phys.* 109, 113501 (2011).
8. J.H. Oh, M. Shin, and M.-G. Jang, *J. Appl. Phys.* 111, 044304 (2012).
9. N. Mingo, *Phys. Rev. B* 68, 113308 (2003).
10. X. Lu and J. Chu, *J. Appl. Phys.* 100, 014305 (2006).
11. M.-J. Huang, W.-Y. Chong, and T.-M. Chang, *J. Appl. Phys.* 99, 114318 (2006).
12. P. Martin, Z. Aksamija, E. Pop, and U. Ravaiolo, *Phys. Rev. Lett.* 102, 125503 (2009).
13. Z. Aksamija and I. Knezevic, *Phys. Rev. B* 82, 045319 (2010).
14. J.E. Turney, A.J.H. McGaughey, and C.H. Amon, *J. Appl. Phys.* 107, 024317 (2010).
15. Z. Tian, K. Esfarjani, J. Shiomi, A.S. Henry, and G. Chen, *Appl. Phys. Lett.* 99, 053122 (2011).
16. W. Liu and M. Asheghi, *J. Appl. Phys.* 98, 123523 (2005).
17. W. Liu and M. Asheghi, *J. Heat Transf.* 128, 75 (2006).
18. N. Mingo, L. Yang, D. Li, and A. Majumdar, *Nano Lett.* 3, 1713 (2003).
19. Z. Sui and I.P. Herman, *Phys. Rev. B* 48, 17938 (1993).
20. A. Paul, M. Luisier, and G. Klimeck, *J. Comput. Electron.* 9, 160 (2010).
21. J.M. Ziman, *Electrons and Phonons: The Theory of Transport Phenomena in Solids* (Oxford: Clarendon, 1962).

22. P.N. Keating, *Phys. Rev.* 145, 637 (1966).
23. G.P. Srivastava, *The Physics of Phonons* (New York: Taylor & Francis Group, 1990).
24. M.G. Holland, *Phys. Rev.* 132, 2461 (1963).
25. M. Asen-Palmer, K. Bartkowski, E. Gmelin, M. Cardona, A.P. Zhernov, A.V. Inyushkin, A. Taldenkov, V.I. Ozhogin, K.M. Itoh, and E.E. Haller, *Phys. Rev. B* 56, 9431 (1997).
26. C. Jeong, S. Datta, and M. Lundstrom, *J. Appl. Phys.* 111, 093708 (2012).
27. N. Mingo and D.A. Broido, *Nano Lett.* 5, 1221 (2005).
28. E.B. Ramayya, L.N. Maurer, A.H. Davoody, and I. Knezevic, *Phys. Rev. B* 86, 115328 (2012).
29. J. Zou and A. Balandin, *J. Appl. Phys.* 89, 2932 (2001).
30. J. Carrete, L.J. Gallego, L.M. Varela, and N. Mingo, *Phys. Rev. B* 84, 075403 (2011).
31. H. Karamitaheri, M. Pourfath, R. Faez, and H. Kosina, *IEEE Trans. Electron Devices* 60, 2142 (2013).
32. Z. Aksamija and I. Knezevic, *J. Comput. Electron.* 9, 173 (2010).
33. H. Karamitaheri, N. Neophytou, and H. Kosina, *J. Appl. Phys.* 113, 204305 (2013).
34. H. Karamitaheri, N. Neophytou, M.K. Taheri, R. Faez, and H. Kosina, *J. Electron. Mater.* 42, 2091 (2013).
35. T. Markussen, A.-P. Jauho, and M. Brandbyge, *Nano Lett.* 8, 3771 (2008).
36. M. Luisier, *Phys. Rev. B* 86, 245407 (2012).
37. D. Donadio and G. Galli, *Nano Lett.* 10, 847 (2010).
38. M.-H. Bae, Z. Li, Z. Aksamija, P.N. Martin, F. Xiong, Z.-Y. Ong, I. Knezevic, and E. Pop, *Nat. Commun.* 4, 1734 (2013).
39. X. Lu, *J. Appl. Phys.* 104, 054314 (2008).
40. K.T. Regner, D.P. Sellan, Z. Su, C.H. Amon, A.J.H. McGaughey, and J.A. Malen, *Nat. Commun.* 4, 16040 (2013).
41. M. Zebarjadi, K. Esfarjani, M.S. Dresselhaus, Z.F. Ren, and G. Chen, *Energy Environ. Sci.* 5, 5147 (2012).